Available online at www.sciencedirect.com

ScienceDirect

Advances in Space Research 57 (2016) 2559–2574

ADVANCES IN SPACE RESEARCH (a COSPAR publication)

www.elsevier.com/locate/asr

Selection of astrophysical/astronomical/solar sites at the Argentina East Andes range taking into account atmospheric components

R.D. Piacentini [a,b,*], B. García [c,d], M.I. Micheletti [b,e], G. Salum [b,f], M. Freire [b], J. Maya [c], A. Mancilla [c], E. Crinó [g], D. Mandat [h], M. Pech [i], T. Bulik [j]

[a] LESyC, IMAE, Facultad de Ciencias Exactas, Ingeniería y Agrimensura, Univ. Nacional de Rosario, Rosario, Argentina
[b] Area Física de la Atmósfera, Radiación Solar y Astropartículas, Instituto de Física Rosario (CONICET-Univ. Nacional de Rosario), Rosario, Argentina
[c] Instituto en Tecnologías de Detección y Astropartículas (CONICET-CNEA-UNSAM), Mendoza, Argentina
[d] UTN Facultad Mendoza, Laboratorio Pierre Auger, Mendoza, Argentina
[e] Facultad de Ciencias Bioquímicas y Farmacéuticas, Univ. de Rosario, Rosario, Argentina
[f] Escuela de Cs. Físicas y Nanotecnología, Yachay Tech, 100119 Urcuquí, Ecuador
[g] Facultad de Ciencias Fisico-Matemáticas, UNSan Luis, San Luis, Argentina
[h] Institute of Physics of Academy of Science of the Czech Republic, Czech Republic
[i] RCPTM, Joint Laboratory of Optics of Palacky University and Institute of Physics of AS CR, Faculty of Science, Palacky University, Czech Republic
[j] Astronomical Observatory, University of Warsaw, Aleje Ujazdowskie 4, 00-478 Warsaw, Poland

Received 23 December 2015; received in revised form 10 March 2016; accepted 12 March 2016
Available online 19 March 2016

Abstract

In the present work we analyze sites in the Argentinian high Andes mountains as possible places for astrophysical/astronomical/solar observatories. They are located at: San Antonio de los Cobres (SAC) and El Leoncito/CASLEO region: sites 1 and 2. We consider the following atmospheric components that affect, in different and specific wavelength ranges, the detection of photons of astronomical/astro physical/solar origin: ozone, microscopic particles, precipitable water and clouds. We also determined the atmospheric radiative transmittance in a day near the summer solstice at noon, in order to confirm the clearness of the sky in the proposed sites at SAC and El Leoncito. Consequently, all the collected and analyzed data in the present work, indicate that the proposed sites are very promising to host astrophysical/astronomical/solar observatories. Some atmospheric components, like aerosols, play a significant role in the attenuation of light (Cherencov and/or fluorescence) detected in cosmic rays (particles or gamma photons) astrophysical observatories, while others, like ozone have to be considered in astronomical/solar light detection.

Keywords: Astrophysical; Astronomical; Solar: sites; Argentina-Andes: atmospheric components

1. Introduction

Astrophysical and astronomical observatories have very demanding requirements on the clear sky conditions and those devoted to the search of astroparticles (ultra-high energy photons and particles) have additional needs in terms of available flat space and an adequate altitude (to be able to detect the maximum development of the cosmic ray showers) for their considered sites.

Astrophysical/astronomical/solar facilities, involve big projects (frequently carried out by giant international collaborations) with special requirements on site selection for their construction. For these kind of facilities, an

* Corresponding author at: LESyC, IMAE, Facultad de Ciencias Exactas, Ingeniería y Agrimensura, Univ. Nacional de Rosario, Rosario, Argentina.
E-mail address: ruben.piacentini@gmail.com (R.D. Piacentini).

http://dx.doi.org/10.1016/j.asr.2016.03.027
0273-1177/

important scientific constraint is to have good quality atmospheric conditions given by the clearness of the atmosphere. Different atmospheric components that contribute to reduce atmospheric transmittance are analyzed in this work for sites in the Argentinian Andean regions, selected in the framework of the site selection process of the Cherencov Telescope Array (CTA) Astroparticle Physics Project. But the results about their atmospheric conditions are of interest also for other astrophysical and astronomical (including solar) applications.

Astroparticle Physics is a relatively new transdisciplinary field of physics, a product of the interaction between particle and nuclear physics, astronomy and cosmology. There is a widespread conception that in the last decade this field of research has become a mature astronomical discipline Hinton et al. (2013). A pillar and strategic topic of its research is high energy messengers (charged particles, neutrinos, gamma rays) and it is apparent that most of the corresponding research projects have been or will be implemented within international collaborations, as has been the case for the Pierre Auger and CTA projects (see Abraham et al., 2004; Aab et al., 2015a; Actis, 2011).

The reconstruction of gamma rays showers is based, for CTA Project, on Cherencov light detection. Moving through the atmosphere at speeds higher than the phase speed of light in air, secondary charged particles (such as electrons and positrons) of the cascade originated by the primary astroparticle, emit a beam of bluish light, known as Cherenkov light. In the last decades, general reviews on the subject show the evolution of the ideas about Cherenkov light detection and the fundamental discoveries (see for example Cawley and Weeks (1996), Ong (1998), Catanese and Weeks (1999), Hinton and Hofmann (2009), Hillas (1985) and Hillas, 2013).

For near vertical showers, this Cherenkov light illuminates a circle with a diameter of hundred of meters on the ground. This light can be captured with optical devices and used to image the shower. Reconstructing the shower axis in space and tracing it back onto the sky, the celestial origin of the cosmic gamma ray is determined.

The Pierre Auger is a hybrid project: composed of surface and fluorescence (SD and FD) detectors, to register both the lateral distribution of the shower at ground level and the shower development across the atmosphere. The latter is detected by the FD system. It registers the fluorescence photons emitted during the passage of the cosmic ray shower through the atmosphere.

Although the Extensive Air showers are common to both, the Pierre Auger Observatory and CTA are different systems of detection, because they observe different energies and phenomena produced at different parts of the atmosphere: fluorescence emission has time scales of microseconds, and depends mainly on the presence of N_2 and water vapor, Cherenkov light is produced in time scales of nanoseconds and depends on the air density in the effective collection area, which is determined by the angle of emission; for gamma photons in the energy range of interest for CTA, the maximum of the shower is between 8 and 12 km asl (with an air density of 200–300 g cm^{-2}), while for high energy particles in the energy range of interest for Auger, this maximum is at about 1.4 km asl, that is almost ground level at the Auger Observatory.

In spite of the differences, the study of the atmosphere for both systems is devoted to the same parameters, with small differences in the requirements.

The Argentina (East) Andes mountains have geographical and climatic (meteorological and solar radiation) conditions that are, in principle, very adequate for the placement of astrophysical/astronomical observatories and Solar facilities. In particular, the Pierre Auger Observatory of ultra-high energy cosmic rays (http://www.auger.org), is located in Pampa Amarilla, a large plateau at about 1400 m asl, near Malargüe city, Province of Mendoza. It consists of about 1700 Surface Detectors (SD) distributed in a ground surface of 30 km×40 km, plus 27 atmospheric Fluorescence Detectors (FD), 24 telescopes in 4 buildings and three high altitude telescopes (the HEAT project), overlooking the array, which observe the longitudinal cosmic ray shower development by detecting the fluorescence light produced by the de-excitation of the atmospheric nitrogen from its excited state originated in its interaction with the charged particles of the shower. The surface detection is based on the Cherenkov light produced when high velocity particles (traveling at speeds higher than the speed of light in the water) interact with the water in the tanks, with time scales of nanoseconds. The Fluorescence Detectors at Auger look for the Nitrogen fluorescence which presents a spectrum partially in the UV and partially in the visible, at a particular line of 337 nm, and a time scale of production of microseconds. The shower maximum is reached between 2 and 8 km asl for a shower with 10^{19} eV, depending on the type and the inclination angle of the primary particle. The FD telescopes of the Pierre Auger Observatory oversee the sky between 0.7 km and 12.5 km above ground level (at about 1.4 km asl), at a distance of 20 km.

The energy for the SD functioning, data collection and transmission is provided by photovoltaic panels. The whole system has been working for more than a decade, showing a good behavior. The FD detectors function connected to the power line, that in all cases was installed especially for this purpose (for details see Aab et al., 2015a,b).

When a large astrophysical/astronomical observatory is proposed to be built for the detection of light, coming from astronomical sources or originated by showers of astroparticles (high energy photons and particles), a detailed search for the best places in the world is undertaken and the clearness of the sky is usually a main condition to be addressed. An essential feature of the CTA, when considering the site selection, is their lack of shelters. Whereas a typical optical telescope is protected from extreme weather by a dome the CTA telescopes are always exposed to the environment. The choice of lack of shelter has been made because of cost. This fact explains the necessity of many of the

environmental requirements. Also, other aspects like geology and accessibility (real and via internet) of the site have to be considered. In the present work, and after a search for several possible places as candidates for CTA, we made a detailed analysis of the following main sites of the Argentina (East) Andes range: San Antonio de los Cobres (briefly SAC, see Section 2.1 for more details) and El Leoncito/CASLEO site (briefly LEO, see Section 2.2). The first one is placed in the Puna of Atacama high altitude desert and the second one near the largest Argentina Optical Observatory (Complejo Astronómico El Leoncito, CASLEO) placed in the Pampa (plateau) of "El Leoncito". We also performed studies at lower altitudes (than the ones of SAC and LEO) with the purpose to characterize completely the region. For this, we consider another site near LEO and we call it LEO++ (see Section 2.2).

The atmosphere is the first detector of an astroparticle. So, in order to select a convenient place for an Astrophysical observatory devoted to the detection of cosmic (or astro) particles (protons, nuclei, elementary particles, gamma photons, and even undiscovered particles), it is of basic importance to analyse the atmospheric constituents, since they contribute in two ways: (i) by interacting with the energetic astroparticle, producing a shower of secondary particles (electrons, positrons, muons, photons, etc.) and (ii) by scattering and absorbing photons of the shower, from the point in the atmosphere where they are generated (normally within the troposphere) to the ground detector. By reconstructing the shower, taking into account the real atmospheric situation, it is possible to find the energy of the primary particle/photon, the arrival direction and the mass composition (in the case of massive particles). Thanks to this information, astroparticles are "messengers" that could reveal the source that emits them (active galactic nuclei, supernova explosions, etc.) or physical processes in the environments of black holes. In the case of cosmic gamma photons of very high energy (in the GeV-TeV range), one of the astrophysical detection techniques that is providing at present, and will give in the future, a large amount of information, is based on the detection of UV, visible and IR (Cherenkov) photons generated by the secondary particles (see for example, the HESS, High Energy Stereoscophic System at http://www.mpi-hd.mpg.de/hfm/HESS/ and the CTA, at www.cta-observatory.org). We present in Section 2 the particular characteristics of the possible sites, for the placement of astrophysical/astro nomical/solar facilities, selected as Argentinean candidates during the site search for the CTA observatory, in Section 3 the ground and satellite results of the time dependence of the atmospheric variables that result the most important ones for the definition of the site to hold this kind of facilities, in Section 4 the ultraviolet and visible photon transmittance of the atmosphere for the day December 22, 2015 (around Southern Hemisphere summer solstice) near noon for clear sky condition and for the three proposed Argentinean sites. In Section 5 we describe the conclusions derived from the present work.

2. Possible astrophysical/astronomical sites of the Argentina (East) Andes range

Argentina has many potential candidate sites satisfying the basic requirements for installation of astrophysical/astronomical observatories. Mostly in the Northwest of the country, in the provinces that lay at the feet of the Andes mountains (Mendoza, San Juan, La Rioja, Catamarca, Salta, and Jujuy) it is possible to find adequate flat areas of about 10 km^2 at height above around 1600 m, with clear skies and suitable meteorological and geographical conditions. After a detailed pre-selection of a dozen promising sites, the search was successively refined by analysis of cartography, available climate data, local surveys and interviews with experts in the search for astrophysical/astronomical sites. We present in what follows three possible sites.

Different techniques can be employed for detection of astroparticles (see for example Abraham et al., 2004; Actis, 2011). The sites (SAC, LEO and LEO++) investigated during the process of the search of the site for the emplacement of the CTA Observatory of the Southern Hemisphere, as well as the Pierre Auger Observatory site, present good atmospheric conditions to hold various astrophysical/astronomical/solar projects, as shown in Section 3.

In the special case of CTA, the site layouts were optimized by the physics and Monte Carlo working groups, and the final array layouts were not decided at the time when the site studies were performed. From the simulations, the Southern array required to have an area of 10 km^2 with minimum extent in all dimensions >3 km. These requirement values were used for the site selection process.

2.1. San Antonio de los Cobres

One of the proposed Argentinean sites is very near San Antonio de los Cobres town (SAC) (24° 02′ 42.7″ S, 66° 14′ 05.8″ W, 3,607 m asl) in the high altitude desertic place of Puna of Atacama, in Salta Province (Fig. 1). In Fig. 2 top we present a satellite image of the NW Argentinean Andes region where the SAC site is placed. Fig. 2 bottom describes the altitudinal profile corresponding to the SAC latitude, showing a small maximum mean slope of about 5 m per kilometer.

In the framework of the CTA project for the detection of ultrahigh gamma photons of GeV-TeV energy, this site was considered as a possible one. After a detailed analysis through astroparticle detection Monte Carlo simulations, sites at lower altitudes (see Section 2.2) were considered to be better for CTA.

2.2. El Leoncito/CASLEO region

In San Juan Province, Argentina, we selected two candidate sites: one in the Pampa of El Leoncito, near CASLEO

Fig. 1. Representation of the Andes region where the selected sites are placed: San Antonio de los Cobres (SAC), El Leoncito region -near CASLEO (Complejo Astronómico El Leoncito)- where two places are considered, LEO and LEO++ (see Sections 2.1 and 2.2) (Google Earth image).

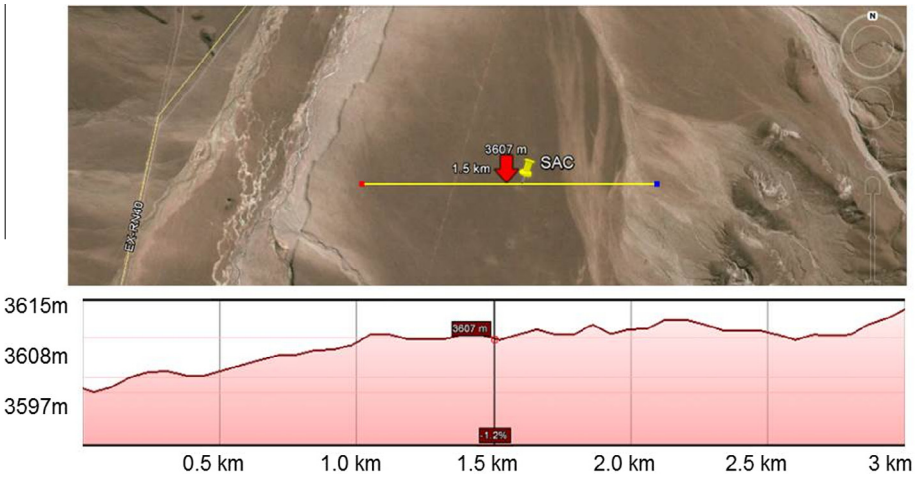

Fig. 2. Top: General satellite view of San Antonio de los Cobres site, with the arrow indicating its position. Bottom: Altitudinal profile at the latitude of San Antonio de los Cobres site. The slope of the area is 1.2% (Google Earth images).

(Complejo Astronómico El Leoncito) (LEO) (31° 04′ 48″ S, 69° 16′ 12″ W, 2672 m asl) and the second one near Calingasta Town, called LEO++ (31° 24′ 22″ S, 69° 29′ 32″ W, 1,630 m asl).

In Fig. 3 top, we present, as for SAC, a satellite image of the West Argentinean Andes region were LEO site is situated. In the same figure we represent at bottom, the soil slope, with a mean maximum value of 83 m per kilometer.

Fig. 4 top shows the location of LEO++ (near LEO) and from Fig. 4 bottom, the altitudinal profile corresponding to the LEO++ latitude can be derived, giving a mean maximum value of 40 m per kilometre.

Both sites are placed at the middle of the region which is limited at the right by the Precordillera and at the left by the Andes mountains (where the LEO site is located) and in Calingasta valley (where the LEO++ site is situated).

3. Atmospheric components (satellite and ground data) analysis for the site selection

The atmosphere is made of different zones determined by the temperature gradient in them, as a function of height: the troposphere (from ground to the tropopause placed at about 8–10 km in the polar regions and 15–18 km at the Equator) where the temperature decreases with height; the stratosphere (from the tropopause to the stratopause located at about 50 km) where the temperature increases with height (due to ozone absorption of solar

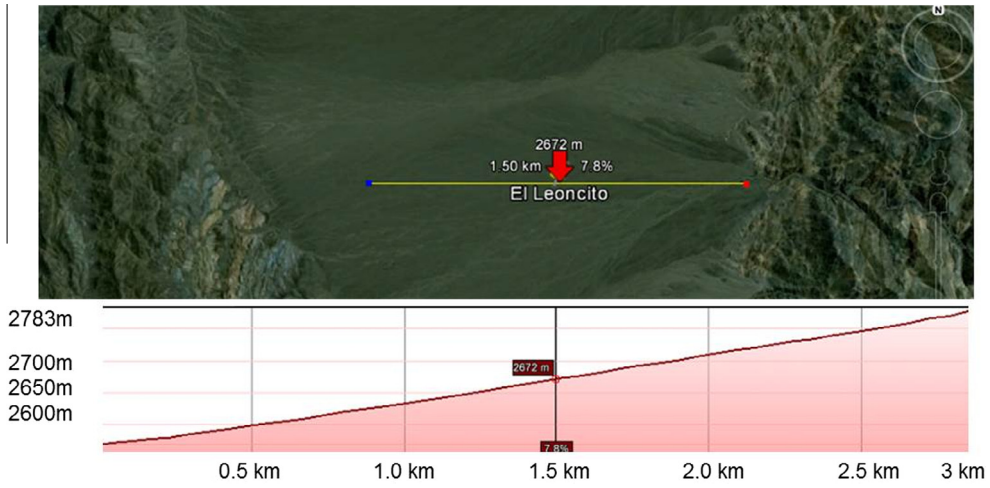

Fig. 3. Top: General satellite view of El Leoncito/CASLEO (LEO) site, with the arrow indicating its position. Bottom: Altitudinal profile at the latitude of the LEO site, The slope of the area is 7.8% (Google Earth images).

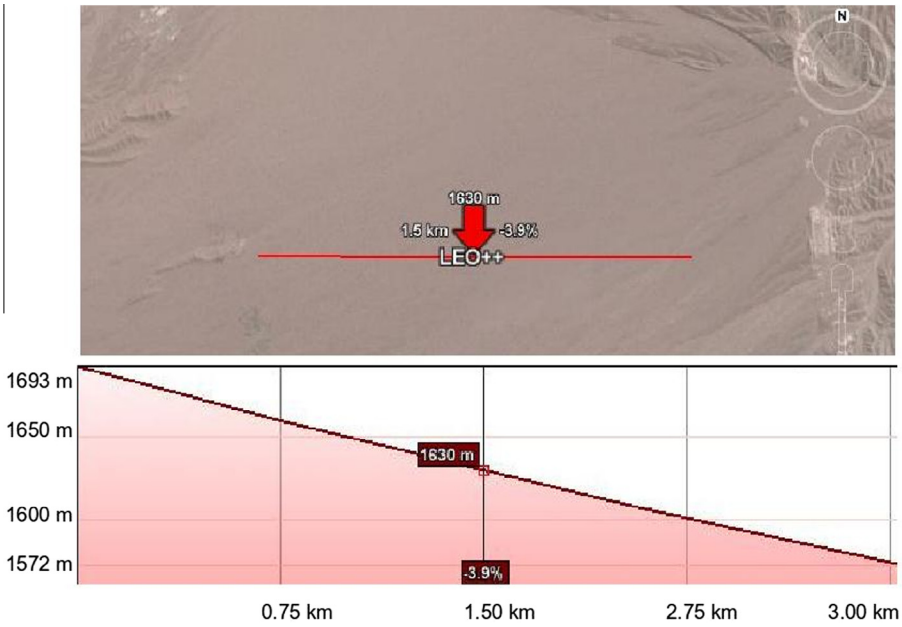

Fig. 4. Top: General satellite view of El Leoncito/CASLEO (LEO++) site, with the arrow indicating its position. Bottom: Altitudinal profile at the latitude of the LEO++ site. The slope of the area is 3.9% (Google Earth images).

light); the mesosphere (from the stratopause to the mesopause at about 80 km) where temperature again decreases with height (since ozone is mostly absent in this layer) and the thermosphere (that extends over the mesopause) where temperature increases with height. Most of the atmospheric components that attenuate the electromagnetic radiation are concentrated in the troposphere and stratosphere. Aerosols, clouds and water vapor are almost completely confined to the troposphere (with scarce and rare exceptions like stratospheric aerosols, for example those of volcanic origin, or stratospheric clouds like the polar ones). The troposphere also contains 90% of atmospheric air. Air molecules, aerosols and clouds are the atmospheric variables that have major incidence in the transmittance of the UV and/or Visible light generated during the passage of cosmic ray showers, like the ones studied in the frame of the CTA and Auger Projects. On the other hand, ozone is located mostly in the stratosphere (and with a significantly less concentration in the troposphere) and its knowledge is necessary to evaluate the total attenuation of light from the top of the atmosphere to ground (for example, for solar or stars light studies and applications in astronomical/solar facilities).

3.1. Aerosols

In relation to the search for a suitable location for the astrophysical H.E.S.S. site, Esposito et al. (2003) analyzed

the aerosol characteristics at the Khomas highlands in Namibia. In a similar but more complete way, we analyzed the behavior of the aerosols in the proposed Argentinian sites, through the aerosol optical depth (from satellite data) and aerosol concentration (from ground measurements). We like to point out that, concerning dust and sand particles suspended in the atmosphere, the requirements for the CTA placement are: "The natural cleanliness class of the site at 3 m above ground should be better than ISO-Class 8 (according to ISO14644-1) for 90% of the time (survival condition). This ISO-Class 8 corresponds to a limit of "29,300 particles of diameter greater than 5 μm per m^3 of air".[1] This specification is mainly motivated for the maintenance of the mirrors from degradation, the scattering particles of the most interest for detection are of a different size than those corresponding to the ISO-Class 8.

3.1.1. Aerosol optical depth from satellite data

The Aerosol Optical Depth (AOD) for a given wavelength enters in astroparticle shower reconstructions, to evaluate the photon attenuation by aerosols. We present AOD_{550} values for the Argentinean sites: SAC, LEO and LEO++, the last two all together since the satellite pixel data is $0.5° \times 0.5°$, including both locations. They are derived from data measured by SeaWiFS instrument on board of SeaStar/NASA satellite, through the improved Deep Blue algorithm. This instrument, is described in the corresponding NASA web page (http://oceancolor.gsfc.nasa.gov/SeaWiFS/SEASTAR/SPACECRAFT.html). The registered wavelengths are in the interval: 402–885 nm and we consider the AOD at 550 nm, since it is commonly used internationally. The incoming solar radiation is collected by a folded telescope and reflected onto a rotating half-angle mirror. It provides contiguous scan coverage at nadir from a 705 km orbital altitude with the SeaWiFS spatial resolution of 1.13 km at nadir. Solar and lunar radiations are used for the SeaWiFS calibration. The detected and amplified signals are routed from the scanner to the electronics module where they are further amplified and then filtered to limit the noise bandwidth. The Goddard Earth Science Data (GES)/NASA Center created a data set by combining the long-running, well-calibrated radiance data from the SeaWiFS mission (1997–2010) and a consistent algorithm to retrieve aerosol properties over both land and ocean. About Deep Blue Aerosol Data, they produce 3 different types of data: daily level 2 (L2), daily level 3 (L3) and monthly level 3 (L3M) products, with a $0.5° \times 0.5°$ and $1° \times 1°$ pixel resolutions.

In Fig. 5 we present the mean daily time series for the 1998–2006 period, measured by the same satellite instrument, at SAC and CASLEO sites, respectively. The mean AOD_λ value and standard deviations are: $AOD_{550nm,SW,SAC} = 0.024 \pm 0.012$ and $AOD_{550nm,SW,CASLEO} = 0.027 \pm 0.021$. They are within the lowest in the world. These values can be compared with those obtained from the same SeaWiFS source: the Paranal Observatory on the other side of the Andes mountains (Chile), presents $AOD_{550nm,SeaWiFS,Paranal} = 0.042 \pm 0.018$ and for the twin Gemini Observatories, the Gemini South, also located in Chile, has $AOD_{550nm,SW,GS} = 0.069 \pm 0.042$ and the Gemini North (placed in Hawaii) has $AOD_{550nm,SW,GN} = 0.052 \pm 0.056$. Concerning the aerosol optical depth for well established solar observatories, the Kitt Peak National Solar Observatory (Arizona, United States) has $AOD_{550nm,SW,KP} = 0.117 \pm 0.112$ and the Observatory of Paris-Meudon has $AOD_{550nm,SW,PM} = 0.177 \pm 0.111$. Another important result is that the maximum mean monthly AOD at SAC is lower than 0.07 and for LEO (and LEO++), lower than 0.1. These very small mean values confirm that no big volcanic eruptions or other effects, like dense aerosol clouds transported by winds, affected the proposed places, in the analyzed period.

3.1.2. Aerosol concentration from ground data

For the study of the aerosol concentration, we employed a GRIMM 1.109 aerosol spectrometer. This instrument measures mass or number concentration for particles with diameter >0.22 μm. It can also determine the concentration contribution for different size intervals in the range 0.22–32 μm (31 intervals or channels within this range). This instrument operates with a constant air flow of 1.2 litre/min; an air sample containing aerosols enters into the device and is led to the measuring cell. A laser diode ($\lambda = 655$ nm) emits light which is scattered by airborne particles. The scattered pulse of every particle in the sample is counted, and the intensity of these scattering patterns can be associated with the particle size. Then by calculations, mass or number distribution can be obtained. Finally the particles are captured by a Polytetrafluoro-ethylene (PTFE) filter for further analysis (gravimetry, optical microscopy, etc.).

The GRIMM was installed near ground level in SAC, El Leoncito/CASLEO (LEO) region and LEO++. At CASLEO it was close to the world network AERONET instrument for aerosol detection (http://aeronet.gsfc.nasa.gov). The collector pipe extreme, was in all the cases at about 2.5 m above the location altitude of the instrument.

The data were collected in the following periods of time: 27th December (4:10 am initial local time, UT - 3 h) to 4th January 2013 (5:35 pm final time) for LEO region, from 6th May (3:32 pm initial time) to 9th May 2013 (3:31 pm final local time) for SAC, and from 9th October 2013 (1:02 pm initial local time) to 23rd October 2013 (1:12 pm final local time) for LEO++. Data have been registered continuously during the mentioned periods in order to have information about concentration values not only during night time (when astrophysical/astronomical observations take place) but during the whole day, as the aerosols not only affect light transmission but also have an abrasive effect detrimental to the mirrors that would then degrade the telescope transmission.

[1] CTA Consortium, Site Evaluation Summary, internal communication, 2014.

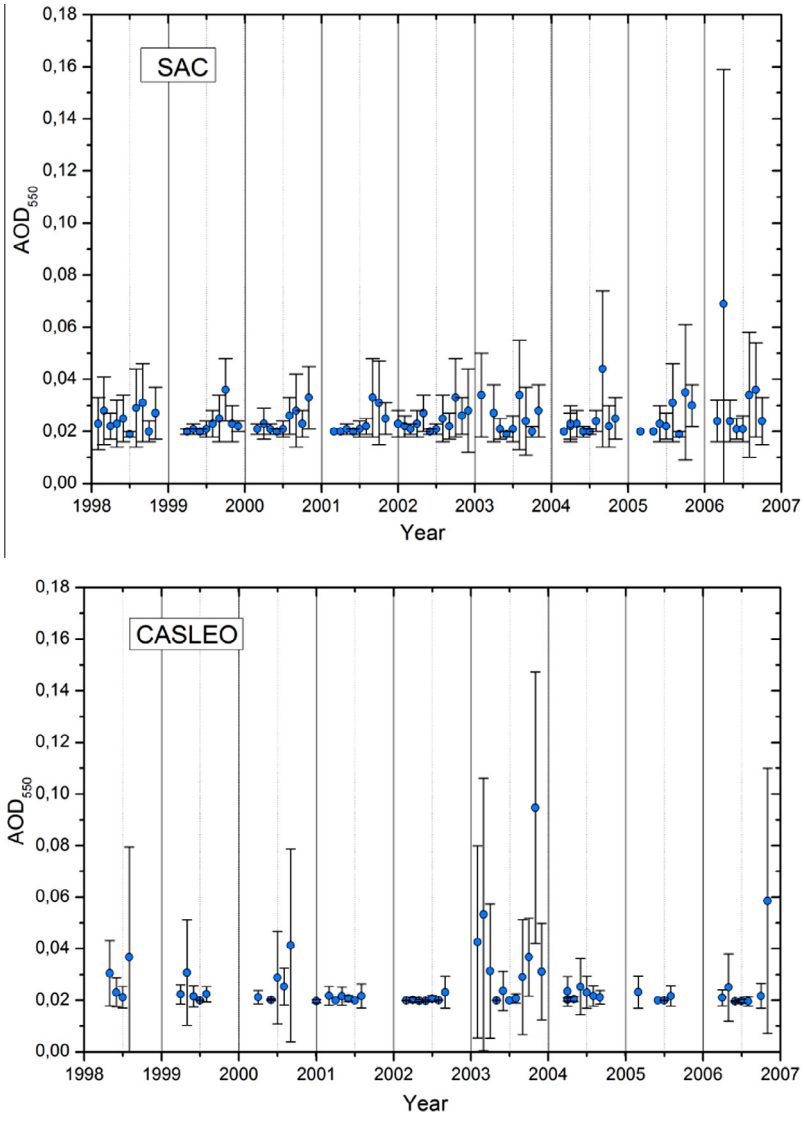

Fig. 5. Area average ($0.5^o \times 0.5°$) daily time series (1998–2006 period) Aerosol Optical Depth at 550 nm (AOD_{550nm}) for: SAC (top) and LEO and LEO++, actually CASLEO (bottom). *Source*: SeaWiFS instrument on board of SeaStar/NASA satellite.

Table 1
Night duration for the corresponding period in each measurement site.

Site	Night duration (local time, UT −3 h)
SAC	9:00 pm–8:00 am
LEO	10:30 pm–7:00 am
LEO++	10:00 pm–7:00 am

The corresponding mean total particle mass concentration and standard deviation equals to (mean + one asymmetric std dev, mean, mean-another asymmetric std dev): (2.7 + 8.5, 2.7, 0) $\mu g\, m^{-3}$ for SAC site, (9.9 + 25.6, 9.9, 0) $\mu g\, m^{-3}$ for LEO site and (8.4 + 22.8,8.4, 0) $\mu g\, m^{-3}$ for LEO++ site. These values correspond to the whole period (day and night time).

For the time period mentioned for each site, we calculate, as displayed in Table 1, the apparent sunset/sunrise time following the algorithm given by NOAA: http://www.esrl.noaa.gov/gmd/grad/solcalc/sunrise.html, which takes into account the diffraction of light effect due to the atmosphere. We also consider a 30–45 min period after/before the apparent sunset/sunrise to assure the absence of diffused sunlight.

A more detailed study of the atmospheric content during night period is very important because it is when measurements at astrophysical/astronomical facilities would take place. We present in Figs. 6–8, the night time mean values of the aerosol mass concentration (measured with the GRIMM instrument) as a function of time. In these figures, the horizontal error bar is centerd on each point and describes the night time duration (according to Table 1), while the vertical error bar is the standard deviation, that can be interpreted as a measure of the concentration fluctuations around the calculated mean value.

The maximum night time mean values of aerosol concentration are lower than 6 $\mu g\, m^{-3}$, 22 $\mu g\, m^{-3}$ and

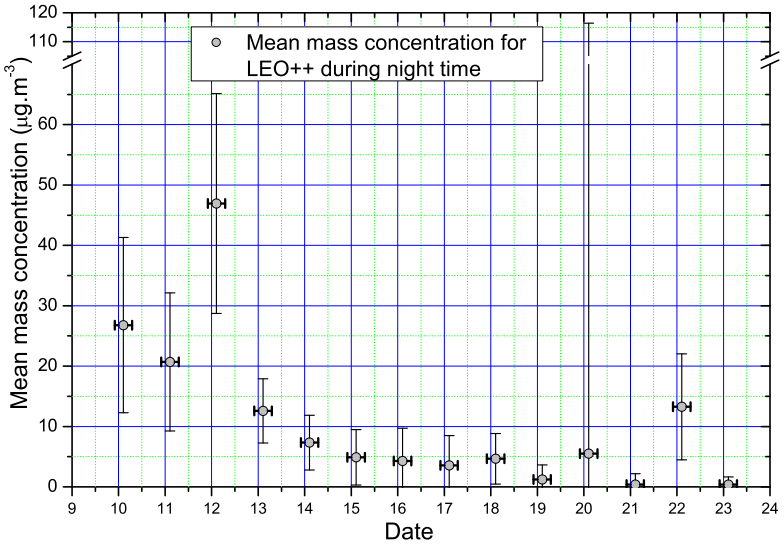

Fig. 6. Mean mass concentration (during night time) for SAC from 6th May (3:32 pm initial time) to 9th May 2013 (3:31 pm final local time).

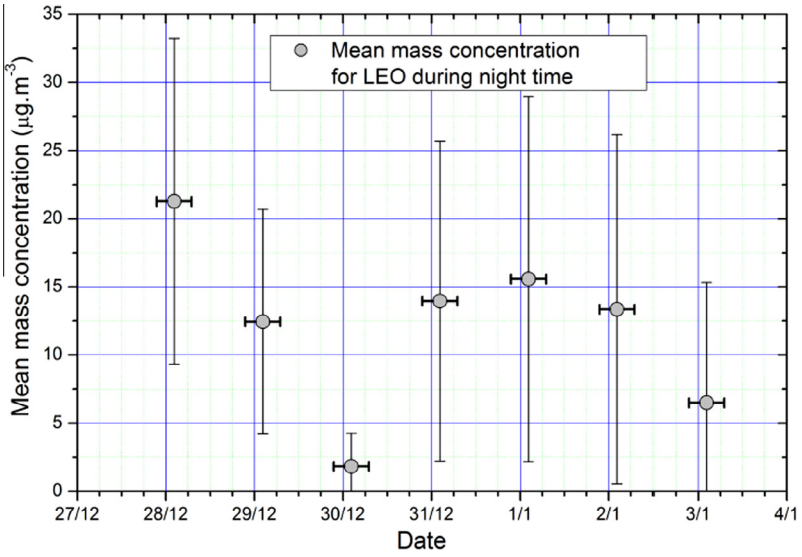

Fig. 7. Mean mass concentration (during night time) for LEO from 27th December 2012 (2:00 pm initial local time) to 4th January 2013 (5:35 pm final time).

48 μg m^{-3}, for SAC, LEO and LEO++, respectively. In order to verify if these concentration values are actually lower than those considered by international astrophysical teams searching for adequate sites, we compare the CTA consortium requirements introduced in Section 3.1, with the latter results. Consequently, by modelization, we transformed the mass concentration values (μg m^{-3}) into particle concentration values (particle.m^{-3})(Mathias Barthel, GIP Messinstrumente Company, Germany, private communication). The corresponding mean particle concentration for the Particulate Matter (PM)(diameter >5 μm) fraction (summarized in Table 2) are: 2800 particles m^{-3} for SAC, 5860 particles m^{-3} for LEO and 8800 particles m^{-3} for LEO++, well below the CTA upper limit described above.

It must be pointed out that the counting efficiency of the instrument is 90%, as was determined by Heim et al., 2008. However, even if two standard deviations are considered (in order to obtain the 95.5% interval range) to the mean values, the corresponding results at the Argentinian sites, SAC, LEO and LEO++, are lower than the CTA upper limit of 29,300 particles m^{-3} (see Table 2). For comparison purposes, we also included in Table 2 the aerosol particle concentration values determined at the Coihueco Fluorescence Detector site, from the Auger astroparticle Observatory (35° 06′ 50″ S, 69° 35′ 59″ W, 1719 m asl) with the same GRIMM instrument, placed at Malargüe, Province of Mendoza, Argentina, in the same East Andes range. These values registered in December 2010 and May 2014 (see Table 2), are larger than those at the new proposed

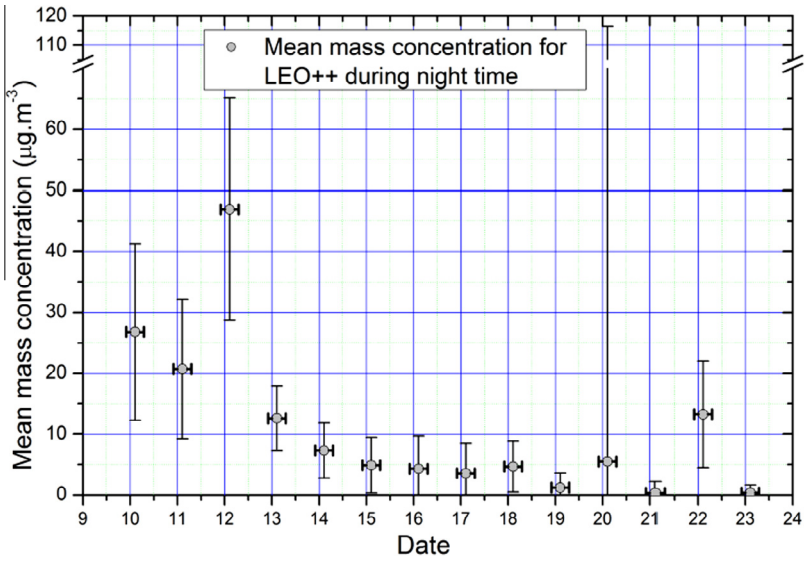

Fig. 8. Mean mass concentration (during night time) for LEO++ from 9th October 2013 (1:02 pm initial local time) to 23rd October 2013 (1:12 pm final local time).

Table 2
Atmospheric particle concentration and error of the mean (std. measured error) at the SAC, LEO and LEO++ proposed sites, measured with the GRIMM 1.109 aerosol spectrometer (range 0.22–32 μm). The same type of data for the Pierre Auger astroparticle Observatory placed at Malargüe, same Andes range, Argentina are also presented for the corresponding months, for comparison purposes. Note: The counting efficiency of the GRIMM instrument is 90%, as was determined by Heim et al. (2008).

SITE	Mean Part. Concent. PM >5 μm (std. error) (particles m^{-3})	PM (diameter >5 μm) below 29,300 part.m^{-3} (%)
SAC	2800(140)	99.38
LEO	5860(70)	99.47
LEO++	8800(100)	90.49
Auger (Dec 2010)	8800(240)	96.05
Auger (May 2011)	14,500(1100)	93.76
Auger (Oct 2011*)	44,700(1200)	67.98

* During this month the eruption of the Chilean Volcán Puyehue-Cordon Caulle produced anomalously large values of the aerosol concentration.

sites. During October of 2011 the eruption of the Chilean Puyehue-Cordon Caulle volcano produced anomalously large values of the aerosol concentration.

Concerning the possibility of volcanic eruptions, the region has active volcanoes, but the aerosol data collected by different satellites like OMI on board of NASA satellites and GOME on ESA satellite, show that the proposed sites of SAC and CASLEO (LEO and LEO++) have almost all days with very low aerosol optical depth values. In particular Piacentini et al. (2012), analyzed the SO_2 space-time evolution in the region and in particular during one of the most intense eruption of the Lascar volcano that took

Table 3
Day and night total aerosol Mean Mass Concentrations (MMC) and corresponding standard deviations (Std. dev.), at the Argentinian sites SAC, LEO and LEO++, for the same periods as given in Fig. 9 for SAC, Fig. 10 for LEO and Fig. 11 for LEO++.

	SAC MMC (std.dev.) μg m^{-3}	LEO MMC (std.dev.) μg m^{-3}	LEO++ MMC (std.dev.) μg m^{-3}
Total day mean	2.2 (0.9)	9.1 (5.0)	6.8 (7.6)
Total night mean	3.4 (1.5)	11.8 (5.9)	10.9 (13.9)

place from the period 18–26 April 1993. The days 19 and 21 of that month, the plumes arrived at San Antonio de los Cobres, but with a decreasing intensity for the consecutive days, as was shown by the aerosol index evolution measured by the TOMS instrument on board of Nimbus 7/NASA satellite. We like to point out that several very large-high quality telescopes are placed in the other site of the Andes, the Chilean Atacama Desert, being this region part of the "Pacific's ring of fire", even when eruptions introducing to the atmosphere a considerable amount of aerosols and gases, like SO_2 that absorbs UV radiation with higher photoabsoption cross section than ozone for wavelengths lowers than about 325 nm (see http://es.scribd.com/doc/91163230/8/UV-SO_2-and-O_3-absorption-spectra), may occur, the period in which they could affect the proposed sites is quite short (Piacentini et al., 2012).

Mean concentration values, as obtained from GRIMM 1.109 measurements performed near the local surface, are lower during the day period than during the night one, for the three proposed sites, as displayed in Table 3. This is in accordance with the effects of the behavior of the planetary boundary layer, which reaches a higher altitude during the hours when the solar radiation heats up the earth surface driving the convection of the air located next to the surface. When heated by the sunlight, this air,

containing most of the atmospheric aerosols, goes up causing a dilution of aerosol concentrations near the surface. At night, air is confined near the surface (as convention processes ceases when the surface cools) and so do the aerosols, leading to an increase of their concentrations. In the rural Andean sites analyzed, the influence of anthropogenic aerosol sources, that could be responsible of day-night pattern, is negligible. The variation along the hours of the day in aerosol concentration is shown in Figs. 9–11. The minimum values are found at noon and afternoon (where the temperature of the land surface reaches its highest values), while a sudden rise in the values occurs in the evening when aerosols fall to lower altitudes.

The aerosol concentration data registered during the campaigns presented in this work are the first ones obtained for the Argentinean sites proposed for the CTA South Observatory. Due to logistic reasons (including the isolation of these rural sites), it was not possible to perform long term measurements (many months or a year cicle) at the selected sites. The short term measurements are shown as a first approximation of typical values of aerosol concentration for these sites at the specific months of the data taking periods. They are compared with mean values of aerosol concentration for the same months at the Auger Observatory. The measurement time period at each site, that range from some days to a couple of weeks, can be

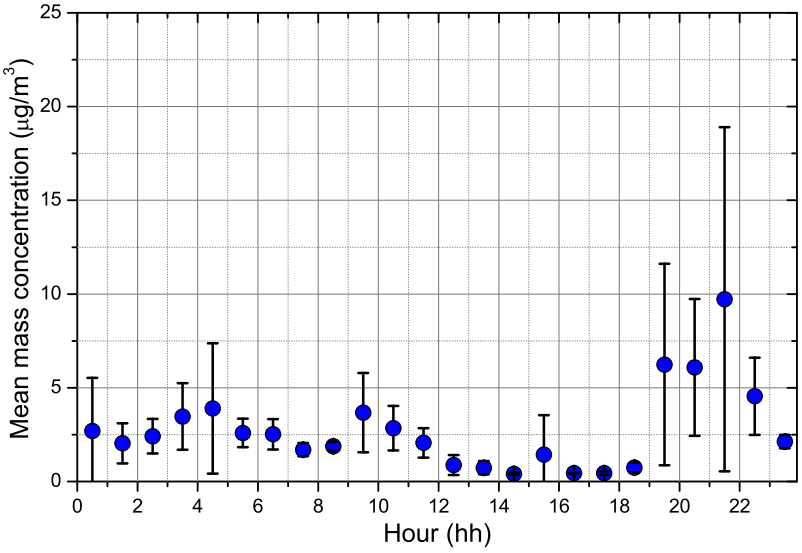

Fig. 9. Hourly variation of the aerosol mean mass concentration per hour for the period of measurement (initial local time: 6th May 2013, 3:32 pm; final local time: 9th May 2013, 3:31 pm) at SAC. Each point is the mean value of all the data registered by the GRIMM 1.109 instrument during every hour period (between two integer hours).

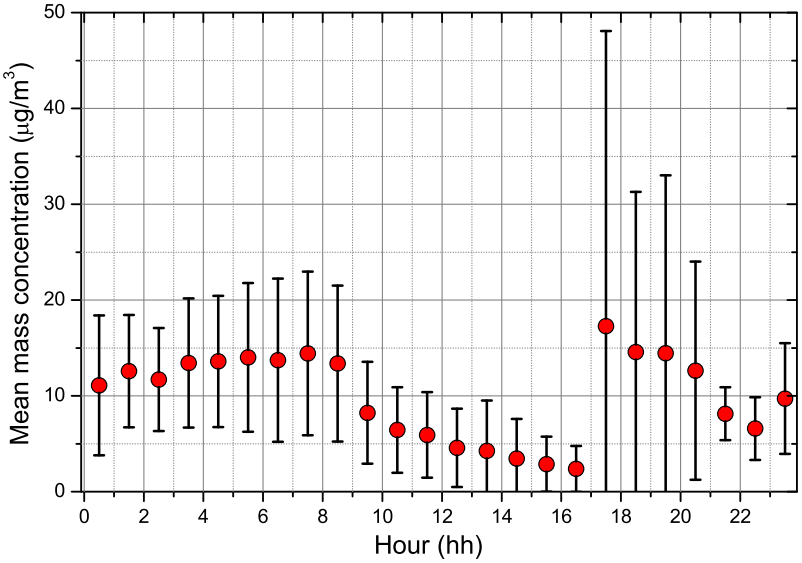

Fig. 10. Hourly variation of the aerosol mean mass concentration for the period of measurement at LEO (initial local time: 27th December 2012, 2:00 pm; final local time: 4th January 2013, 5:35 pm).

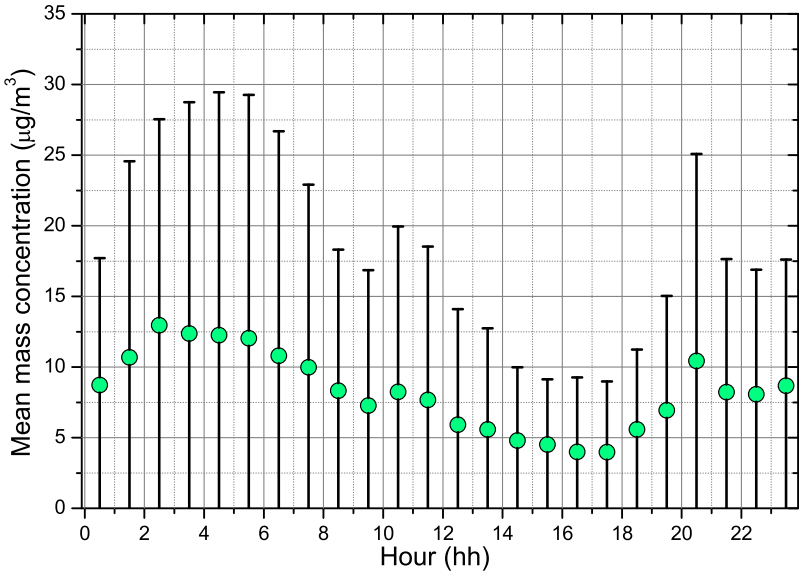

Fig. 11. Hourly variation of the aerosol mean mass concentration for the period of measurement at LEO++ (initial local time: 9th November 2013, 1:02 pm; final local time: 23rd November 2013, 1:12 pm).

considered short in comparison with the whole month but it is still long enough in relation with the aerosol time scale variation that can occur in hours or in less than an hour, depending on weather factors (like wind, precipitation, temperature) as well as on sources, evolution (driven by different processes like nucleation, coagulation, aggregation, deposition), transport, etc. In a days or weeks scale, many of these effects take place, contributing with different signs, so they can approximately cancel out and the mean aerosol concentration value of these periods can be considered as an acceptable estimation of the corresponding mean value of the whole months (that shows the stable tendency of the aerosol situation for these months). For this reason it is valid to compare mean concentration values of the same months of different years and sites, as they can be considered as characteristics of each month for the specific site, since short time scale fluctuations are already balanced out, as explained, and long term variations happen in longer time scales, as for different months along the year when weather variables, sources, etc. experience an appreciable definite tendency in their mean values.

3.2. Ozone (and solar constant) from satellite data

Ozone total column was extracted form the data base determined by the OMI and LMS instruments on board of Aqua/NASA satellite. In particular from Giovanni/NASA AIRXSTM v006 data web page http://giovanni.gsfc.nasa.gov/giovanni/. For SAC the mean considered value is 0.249 cm and for CASLEO (LEO and LEO++ sites) 0.278 cm (as given in Table 4).

Ozone is of importance in the attenuation of solar photons, totally in the FUV (100–280 nm) range and partially in the NUV (280–320 nm) range. So, the location of the sites at high altitudes reduce its total column and consequently increase the possibility to detect electromagnetic radiation in the NUV range, coming from stars, mainly the Sun.

Concerning the extraterrestrial total solar irradiance, commonly named solar constant, it was obtained from the very precise TIM (Total Irradiance Monitor) instrument on board of the SORCE/NASA satellite (http://lasp.colorado.edu/data/sorce/tsi_data/daily/sorce_tsi_L3_c24h_latest.txt), for the day considered in the calculation of atmospheric transmittance (see Section 4).

3.3. Precipitable Water from satellite data

Another quantity of interest in the selection of astrophysical and astronomical sites is the Precipitable Water Vapour (PWV), which is the available H_2O in an ideal atmospheric column at a given place. It starts to absorb at about 700 nm (see Ristori, 2012), consequently, for the

Table 4
Atmospheric components considered for the calculation of the transmittances presented in Fig. 14a–d.

Data	SAC	LEO	LEO++
Latitude (degree)	−24.5	−31.08	−31.41
Longitude (degree)	−66.24	−69.27	−69.49
Altitude(m)	3607	2672	1630
Precipitable water* (cm)	0.53	0.73	0.73
Total Ozone (cm)	0.249	0.278	0.278
CO_2 (ppm)	398.8	398.8	398.8
Solar constant (W m^{-2})	1361.3	1361.3	1361.3
Atmosphere kind	Desert	Desert	Desert
AOD_{550nm}	0.025	0.026	0.026
Albedo	0.06	0.06	0.06

* For precipitable water see Section 3.3.

Table 5
Monthly mean variation of the Precipitable Water Vapor (PWV) of the atmosphere at the proposed Argentinian sites of SAC and CASLEO (LEO and LEO++). The annual mean is given in the last line and corresponds to 22 years average of Surface Meteorology and Solar Energy/NASA satellite data (https://eosweb.larc.nasa.gov/cgi-bin/sse/sse.cgi?skip@larc.nasa.gov). The uncertainty of the measurements is estimated by SSE/NASA in 20% (Mary Jane Saddington, SSAI, NASA Langley ASDC User Services, private communication).

Month	SAC	CASLEO
January	1.10	1.11
February	0.98	1.09
March	0.83	1.02
April	0.47	0.72
May	0.28	0.56
June	0.23	0.53
July	0.22	0.45
August	0.25	0.46
September	0.28	0.53
October	0.40	0.62
November	0.55	0.77
December	0.81	0.94
Mean	0.53	0.73

case of the Cherenkov Telescope Array with photomultipliers that have quantum efficiencies up to about the latter wavelength, in principle, it is not of direct interest for gas absorption of the Cherenkov photons through the atmosphere. Also, it could affect the quality of the telescope mirrors, those at the HighEnergy Stereoscopic System (HESS) astrophysical site (http://www.mpi-hd.mpg.de/hfm/HESS/) degrade at a rate of 3–4% per year (Bernlöhr, 2000) due to wind blown dust erosion and the CTA mirrors will test various technologies in an attempt to lessen this effect (Foerster et al., 2013a). These technologies may suffer other systematic effects relating to ambient environment, for instance the painted surface on the mirrors for solar reflectors degradation depends partially on the water content (see Girarda et al., 2015).

Among several characteristics which determine the quality of a reflective surface, the reflectivity, as well as their stability over time, is one of the most important. It is given by the fabrication technique and the coating material, and it should be maximized between 300 and 450 nm. Current experiments use: mirrors of pure polished aluminum surfaces (Doro et al., 2008), mirrors with aluminum as a reflective material (Bernlöhr, 2003) and with protective layers to ensure resistance against weather conditions (Roache et al., 2008), and glass mirrors with dielectric coating (Foerster et al., 2013b).

The large water content, also could produce the metal corrosion of the structure. Even more, if the amount of precipitable water vapor in the atmosphere is big enough, the humidity of the atmosphere would prevent observation.

A recent study (Dipold et al., 2016) using a dedicated facility built at one of the Argentinean candidate sites to host the CTA Southern array, SAC, monitored the basic mechanical and optical performance of the mirrors and studied the behavior of the mirrors in the presence of water vapor condensation not only on the mirror reflectivity, but also on the image quality. The authors, developed a method to identify condensation in mirror pictures and obscure areas in mirrors facets and concluded that at SAC, dielectric mirrors would have at least 20% of their area obscured for about 2% of the operational time, while the aluminum mirrors would have at most 20% of their area obscured for about 6% of that time.

We display in Table 4 the annual averaged total column precipitable water at the three Argentinian sites. Table 5 shows the monthly variation of this atmospheric variable, with a maximum in January (summer in the Southern Hemisphere) and a minimum in July (winter in the Southern Hemisphere).

For this study, the PWV was estimated through the analysis of NASA/Surface Meteorology and Solar Energy (SSE) data based on a mean of 22 years of satellite measurements (https://eosweb.larc.nasa.gov/cgi-bin/sse/sse.cgi?skip@larc.nasa.gov). This quantity presents the annual mean lowest value at SAC, followed by CASLEO/El Leoncito (which includes LEO and LEO++, since the pixel is $1° \times 1°$), as can be seen in Table 4. The PWV mean value at SAC is 37.7% lower than that at LEO and LEO++. These values can be compared with the results presented by Iqbal (1983) of the PW total column. For a place at 2 km altitude, the annual mean PW value is 0.82 cm and for a higher altitude of 4 km, the annual mean PW value is 0.30 cm.

3.4. Ground data cloud coverage measured at night

The Institute Joint Laboratory of Optics of Palacky University and Institute of Physics CAS developed the All Sky Camera (ASC) hardware and the corresponding software, as a universal device for the monitoring of the night sky quality (Mandat et al., 2015). The ASC system (see Fig. 12) consists of an astronomical CCD camera, a fish eye lens, a control computer and associated electronics. The measurement was carried out during astronomical

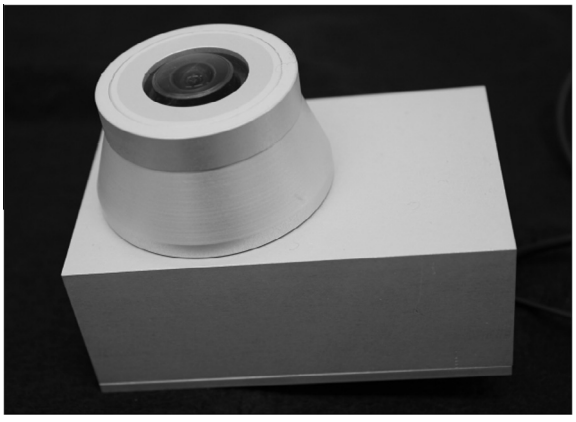

Fig. 12. All sky camera employed in the measurement of the cloud coverage at the SAC, LEO, LEO++ sites.

night (the time when the sun is at least 15 degrees below horizon).

The images are automatically taken for LEO every 5 min (10 min respectively for SAC and LEO++ that used a different ASC hardware) minutes and automatically processed using the control computer of the device. To estimate the Cloud Fraction (CF) we investigate the presence of stars in the field of view of the camera and compare the position with catalogue. We take the visual magnitudes of the stars from the Yale Bright Star Catalogue BSC5. The angular limit of detected and catalogue stars is up to 1°. The ratio of undetected/catalogue stars gives the CF of the night sky and is an estimation of the percentage of the sky that is covered by clouds. It ranges from 0 (all stars from the catalogue are detected) to 1 (all stars from the catalogue are undetected; the sky is fully covered by clouds). Typically, we check about 500 catalogue stars for the whole observed sky, up to 60° operating zenith angle. The error of the algorithm is ±2% for cloudiness <20% (clear sky) and ±5% for cloudiness >80% (cloudy). Problematic images (caused by fresh fallen snow covering the lens, fog, frost) were considered as affected and were not taken into account in the final CF calculation: that limits the clear sky view. The percentage of affected images is 17%, 2% and 2% respectively for SAC, LEO and LEO++ sites. Measurements were made in the periods February 14, 2012 – October 3, 2013, November 15, 2012 – November 4, 2014, and October 8, 2013 – November 14, 2014 at SAC, LEO and LEO++ respectively.

Fig. 13 shows the cumulative distribution of CF of all sites. The red straight dashed line is the CTA criterium for clear sky (CF < 0.2). As we acquire one image each five minutes, and only during the moonless nights, we have, in principle, the percentage of good images, but also the percentage of good observation time (but the time is different for all sites): good means that we have images that could not be analyzed (water on lens, snow etc).

According to the CTA requirement of CF ⩽ 0.2, SAC is the best site from all the analyzed, but for CF ⩽ 0.1 (i.e. a better fraction of clear sky) the LEO site clear time of 80% is much better than the SAC and LEO++ value of 70% of observation time.

In terms of cloud cover, more than 85% of the measurement time was considered as clear sky nights for SAC and for CASLEO the values are over the 78%. These results are in agreement with those obtained by Martinis et al. (2013) for LEO, using a similar instrument and star detection, but a different method to analyse the data and to estimate the cloud coverage.

3.5. Night sky brightness

In order to have confident values for the luminance or the surface brightness of the sky, the night sky brightness (NBS), one of the parameters between the requirements for Astrophysical sites, several studies in the proposed sites for CTA were performed. Aubé et al. (2014) used two different techniques to sample the sky brightness of El Leoncito and LEO++. The first one uses the well known Unihedron's Sky Quality Meter (SQM), which measures the V magnitude inside a large field of view of about 20°; the second technique uses the SAND-4 spectrometer, a low resolution long slit spectrometer (spectral resolution of 1 nm) having a much more restricted field of view. From these observations the authors conclude that the sky background brightness Results 21.6 ± 0.4 mag/arcsec^2 for El Leoncito, 21.7 mag/arcsec^2 for LEO++, and El Leoncito was distinguished for its lower average radiance (especially for the 569 nm line), for characteristics such as the very low presence of aerosols (lower extinction), and for the presence of the mountains to reduce the impact of the surrounding luminous halos.

The NSB for SAC results of 21.9 mag/arcsec^2 (see De la Vega et al., 2014). While the observations at the sites were

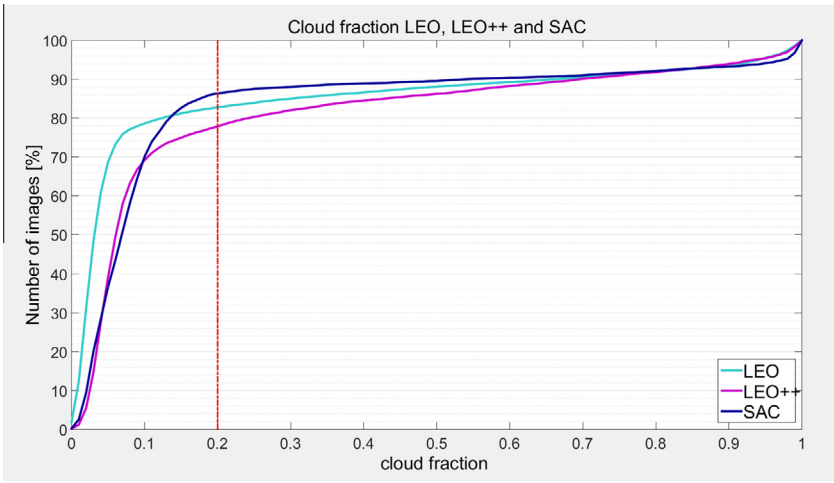

Fig. 13. Distribution of the Cloud Fraction during the observation time at the SAC, LEO and LEO++ sites (0 corresponds to clear sky and 1 to completely fully covered sky). The red dashed line is the limit for the cloudless night sky (CF < 0.2), eg. more than 85% of the observation time CF < 0.2 (cloudless nights) at SAC. (For interpretation of the references to color in this figure legend, the reader is referred to the web version of this article.)

made using the SQM normal filter, centered around the Johnson-V filter wavelength, measurements performed with a Johnson-B filter at El Leoncito and LEO++ resulted in an average of 23 mag/arcsec^2 (De la Vega et al., 2014).

Both sites are within the CTA Consortium requirements, and the requirement for any astrophysical/astronomical observatory, it means a site with NSB of 21.5 mag/arcsec^2 or better in the Johnson-V filter.

4. Ultraviolet and visible photon transmittance

The different components of the atmosphere contribute in a different way to the atmospheric transmittance of UV and visible photons as function of wavelength (Bernlöhr, 2000). Considering the atmospheric components given in Table 4 for the three Argentinian sites, we display in Figs. 14a–c the UV and visible transmittance determined employing the SMARTS algorithm (Gueymard, 1995), for the day 22 December 2015, near the Southern Hemisphere summer solstice at solar noon for clear sky (no clouds) conditions. We can see that, starting the analysis at the lowest wavelengths displayed in the figures, ozone has a large cut-off in the 280–320 nm, then the scattering due to atmospheric gas molecules and aerosols (Rayleigh and Mie scatterings), and finally for wavelengths greater than around 570 nm, water vapor starts to contribute. For Astrophysical observatories, the molecular and aerosol atmospheric components are the most important ones in the contribution to atmospheric attenuation, since normally there is a negligible contribution of Cherenkov and fluorescence photons in the NUV range. In the case of astronomical observatories, the ozone strong cut-off in this wavelength range determines the limit of observation of solar (stellar) photons, traversing the atmosphere from the top to the ground level.

In Fig. 14a–c, we display the corresponding transmittance for each site of the different atmospheric compounds: water vapor, ozone and aerosol and those for the Rayleigh scattering (contribution) and for the total (summed)

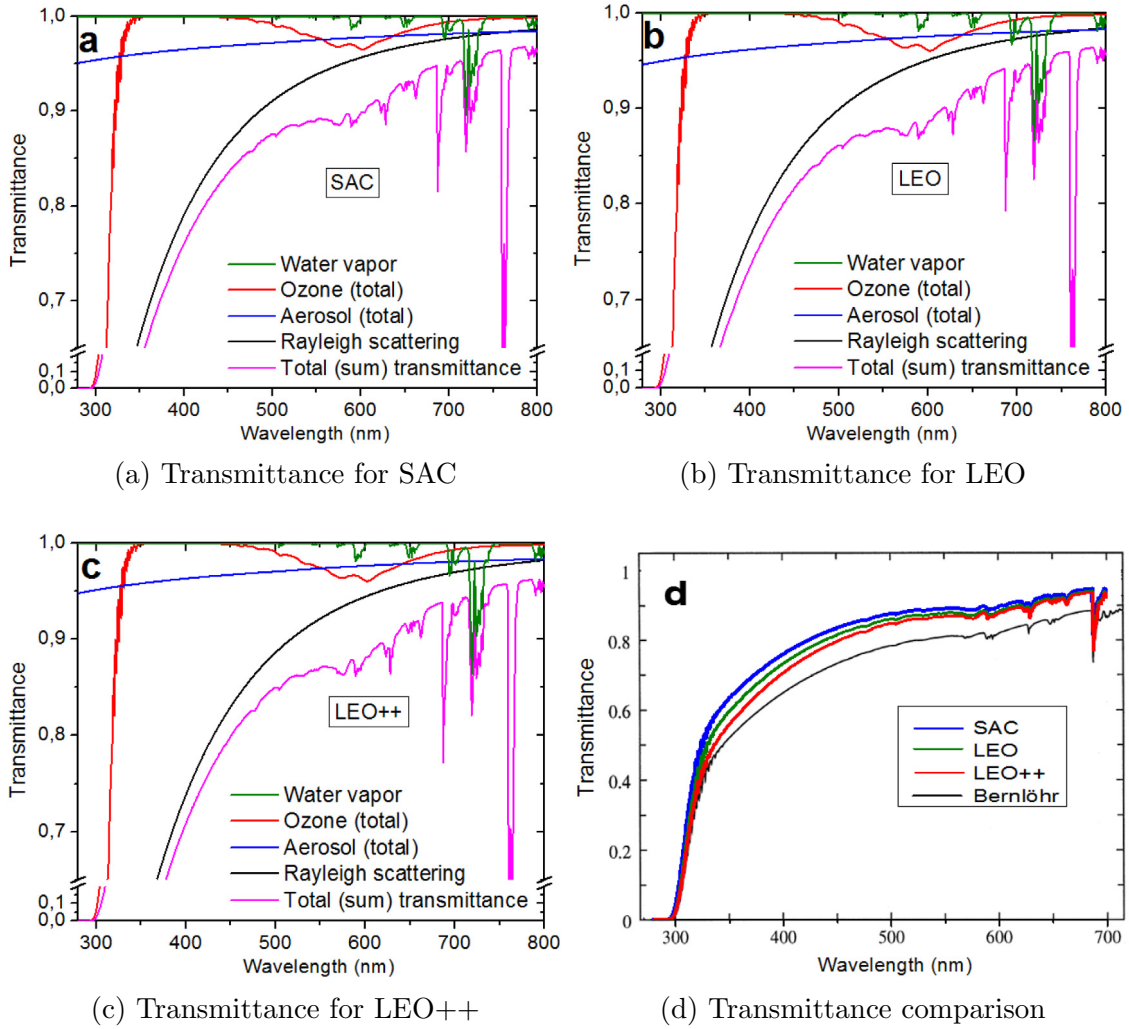

(a) Transmittance for SAC

(b) Transmittance for LEO

(c) Transmittance for LEO++

(d) Transmittance comparison

Fig. 14. Model calculation of the UV and Visible transmittance at the Argentinean (a) SAC, (b) LEO and (c) LEO++ sites, the day 22 December 2015 near noon for clear sky conditions, determined employing the SMARTS algorithm (2.9.5 version), for the atmospheric quantities as given in Table 4, and (d) Total (sum) transmittance for each Argentina Andes place (as given in figures a, b and c) and similar transmittance determined by Bernlöhr (2000).

transmittance due to the incidence of the direct radiation. The SAC ozone transmittance is higher than the LEO and LEO++ transmittances. In the cases of water vapor and Rayleigh scattering transmittances, the behavior of the three sites is very similar. Fig. 14d (bottom right) compare the three total transmittances for the three different analyzed site (SAC, LEO and LEO++) and the direct transmittance of light from a source placed at 100 km of altitude calculated with the MODTRAN model by Bernlöhr (2000), SAC has the largest transmittance, as expected due to its altitude and clear sky, then LEO and finally LEO++, this last one placed at the lowest altitude. Since the concentration of atmospheric components (gases, ozone and aerosol) is very low at the Argentinian sites due to their altitude and latitude, the transmittance in all sites are relatively large compared with that given in the work of Bernlöhr (2000).

5. Conclusions

We summarize in what follows, the atmospheric data obtained in the previous items, in relation with the possibility to place astrophysical/astronomical observatories and solar spectral analysis facilities in the East Argentinian Andes Mountains:

- Aerosol (satellite data): The mean AOD (at 550 nm) value measured with the SeaWiFS/SeaStar NASA satellite at SAC and CASLEO sites are lower or equal to 0.027, being within the lowest in the world. For comparison purposes, the Paranal Observatory in the West side of the Andes mountains has a AOD (at 550 nm) of 0.042. Another important result is that the maximum mean monthly AOD at SAC is lower than 0.07 and for LEO and LEO++, lower than 0.1.
- Aerosol (ground data): The three Argentinean sites have very low total aerosol concentration values, derived from GRIMM aerosol spectrometer measurements at the SAC and CASLEO Argentinean proposed sites. The particle concentration at SAC (2800 particles m^{-3}), LEO (5860 particles m^{-3}) and LEO++ (8800 particles m^{-3}) are smaller than the ISO Class 8 classification of clean ambient (29,300 particles m^{-3}), considered as a maximum limit for CTA. The aerosol concentration measurements are the first ones performed at the proposed sites.
- Ozone (satellite data): The East Andes Argentinian sites have rather low values of ozone total column of 0.249 cm for SAC and 0.278 cm for CASLEO (LEO and LEO++), the latter being 10.4% bigger that the former. It was measured with the OMI and LMS instruments on board of Aqua/NASA satellite.
- Clouds (ground data): The amount of time the cloud fraction is below 0.2 in all the proposed sites, as determined by the ASC instrument, is 87% for SAC, 83% for LEO and 77% for LEO++. These values are comparable to those obtained for other astrophysical sites.
- The night sky background brightness Results 21.36 mag/arcsec^2 for El Leoncito (in agreement with the data obtained for CASLEO) and 21.9 mag/arcsec^2, for SAC. Both sites are within the requirement for Astrophysical observatories.
- Precipitable water (satellite data): As given in the NASA/Surface Meteorology and Solar Energy (SSE) data base, SAC has the lowest value (0.53 cm) and it is 37.7% lower than CASLEO/El Leoncito region value (0.73 cm), which includes LEO and LEO++ sites.

Consequently, all the collected and analyzed data in the present work, indicate that the proposed sites are very promising to host astrophysical and/or astronomical observatories and solar facilities.

Acknowledgements

The authors acknowledge the very detailed pre-review work done by Drs. Michael Daniel and Lluís Font Guiteras of the Cherenkov Telescope Array Collaboration, that contributed to improve the present article.

The support from MINCYT, CONICET, CNEA and National Universities of Rosario and San Luis is also appreciated. Also, to the SEAWiFS and SSE NASA Science Team and to the OMI/KMNI Science Teams for maintaining and improving a large database. The authors gratefully acknowledge the support by the projects LO1305, LE13012, LG14019 and 7AMB14AR005 of the Ministry of Education, Youth and Sports of the Czech Republic.

References

Aab, A., the Pierre Auger Collaboration, 2015a. The Pierre Auger cosmic ray observatory. Nucl. Instr. Methods Phys. Res. A 798, 172–213.

Aab, A., the Pierre Auger Collaboration, 2015b. Searches for anisotropies in the arrival directions of the highest energy Cosmic rays detected by the Pierre Auger Observatory. Ap. J. 804, 15.

Abraham, J., the Pierre Auger Collaboration, 2004. Properties and performance of the prototype instrument for the pierre auger observatory. Nucl. Instr. Methods Phys. Res. A 523, 50–95.

Actis, M. et al., 2011. for a CTA consortium, design concepts for the Cherenkov telescope array. Exp. Astron. 32, 193–316.

Aubé, M., García, B., Fortin, N., Turcotte, S., Mancilla, A., Maya, J., 2014. Evaluation of the sky quality at two Argentinian Astronomical Sites. In: PASP 126 (945), 1068–1077.

Bernlöhr, K., 2000. Impact of atmospheric parameters on the atmospheric Cherenkov technique. Astropart. Phys. 12, 255–268.

Bernlöhr, K. et al., 2003. The optical system of the H.E.S.S. imaging atmospheric telescopes system. Part I. Astropart. Phys. 20, 111–128.

Catanese, M., Weeks, R.C., 1999. Very high energy gamma-ray astronomy. Publ. Astron. Soc. Pac. 111, 1193–1222.

Cawley, M.F., Weeks, T.C., 1996. Instrumentation for very high energy gamma-ray astronomy. Exp. Astron. 6, 7–42.

De la Vega, G., García, B. Maya, J., Mancilla, A., Rosemblant, E., 2014 CTA Studies for characterization of sites in argentina: a contribution on sky background brightness, ITeDA-Internal Technical Note.

Dipold, J., Medina, M.C., García, B., Rasztockyc, E., Mancilla, A., Maya, J., Larrarte, J.J., de Souza, V., 2016. On-site mirror tests for Cherenkov telescopes for the, Cherenkov telescope array. Nucl. Phys. B.

Doro, M., Bastieri, D., Biland, A., Dazzi, F., Font, L., Garczarczyk, M., Ghigo, M., Giro, E., Goebel, F., Kosyra, R., Lorenz, E., Mariotti, M., Mirzoyan, R., Peruzzo, L., Pareschi, G., Zapatero, J., 2008. The reflective surface of the MAGIC telescope. Nucl. Instr. Methods Phys. Res. A 595, 200–203.

Esposito, F., Mari, S., Pavese, G., Serio, C., 2003. Diurnal and nocturnal measurements of aerosol optical depth at a desert site in Namibia. Aerosol Sci. Technol. 37 (4), 392–400.

Foerster, A. et al., 2013a. Mirror development for the Cherencov telescope array. In: Proc. 33rd ICRC; ibid arXiv:1307.4563.

Foerster, A. et al., 2013b. Dielectric coating for IACT mirrors. In: Proc. 33rd ICRC; ibid arXiv:1307.4557.

Girarda, R., Delorda, C., Disdiera, A., Raccurta, O., 2015. Critical constraints responsible to solar glass mirror degradation. Energy Procedia 69, 1519–1528.

Gueymard, C.A., 1995. SMARTS, A simple model of the atmospheric radiative transfer of sunshine: algorithms and performance assessment. Technical Report No. FSEC-PF-270-95. Cocoa, FL: Florida Solar Energy Center.

Heim, M., Mullinsb, B.J., Umhauera, H., Kasper, G., 2008. Performance evaluation of three optical particle counters with an efficient multi-modal calibration method. Aerosol Sci. 39, 1019–1031.

Hillas, A.M., 1985. Cerenkov light images of EAS produced by primary gamma. In: En, F., Jones, C. (Eds.), International Cosmic Ray Conference, pp. 445–448.

Hillas, A.M., 2013. Evolution of ground-based gamma-ray astronomy from the early days to the Cherenkov Telescope Arrays. Astropart. Phys. 43, 19–43.

Hinton, J., Hofmann, W., 2009. Teraelectronvolt Astron. Ann. Rev. Astron. Astrophys. 47, 523–565.

Hinton, J., Sarkar, S., Torres, D., Knapp, J. (Eds.), 2013. Astroparticle Physics, Special Issue, Seeing the High Energy Universe with the Cherenkov Telescope Array: The Science Explored with the CTA, 43.

Iqbal, M., 1983. An Introduction to Solar Radiation, vol. 91. Academic Press.

Mandat D., Miroslav P., Miroslav, H., Schovanek, Miroslav Palatka, Michael Prouza, Petr Travnicek, Janecek,P., Ebr, J., Doro, M., Gaug, M., for the CTA Consortium. 2015. All sky camera for the CTA atmospheric calibration work package. In: EPJ Web of Conferences 89 03007. http://dx.doi.org/10.1051/epjconf/20158903007.

Martinis, C., Wilson, J., Zablowski, P., Baumgardner, J., Aballay, J.L., García, B., Ristori, P., Otero, L., 2013. A New Method to Estimate Cloud Cover Fraction over El Leoncito Observatory from an All-Sky Imager Designed for Upper Atmospheric Studies, vol. 125. PASP, Univ.Chicago Press, pp. 56–67.

Ong, R., 1998. Very high-energy gamma-ray astronomy. Phys. Rep. 305, 93–202.

Piacentini R.D., Crino, E., Ipiña, A., Micheletti, M.I., Salum, G., 2012. Sulfur dioxide and particulate matter produced by volcanic emissions and other events in proposed CTA sites. Technical Note CTA Argentina, September 2012.

Ristori, P., Otero, L., Ballesteros, P., Suárez, A., Medina, C., García, B., Piacentini, R.D., Crino, E., Ipiña, A., Micheletti, M.I., Salum, G., Etchegoyen, A., Quel E., 2012. Precipitable water from ground and satellite data for the Argentinean and Namibian pre-selected CTA sites. Technical Note CTA Argentina. 03–2012.

Roache, E. et al., 2008. Mirror facets for the veritas telescopes. Proc. 29th Int. Cosmic Ray Conf. vol. 3, 1397–1400.